AEM
Journals.ASM.org

Diversity and Expression of RubisCO Genes in a Perennially Ice-Covered Antarctic Lake during the Polar Night Transition

Weidong Kong,[a] David C. Ream,[b] John C. Priscu,[c] and Rachael M. Morgan-Kiss[b]

Department of Medicine, University of California, San Francisco, California, USA[a]; Department of Microbiology, Miami University, Oxford, Ohio, USA[b]; and Department of Land Resources and Environmental Sciences, Montana State University, Bozeman, Montana, USA[c]

The autotrophic communities in the lakes of the McMurdo Dry Valleys, Antarctica, have generated interest since the early 1960s owing to low light transmission through the permanent ice covers, a strongly bimodal seasonal light cycle, constant cold water temperatures, and geographical isolation. Previous work has shown that autotrophic carbon fixation in these lakes provides an important source of organic matter to this polar desert. Lake Bonney has two lobes separated by a shallow sill and is one of several chemically stratified lakes in the dry valleys that support year-round biological activity. As part of an International Polar Year initiative, we monitored the diversity and abundance of major isoforms of RubisCO in Lake Bonney by using a combined sequencing and quantitative PCR approach during the transition from summer to polar winter. Form ID RubisCO genes related to a stramenopile, a haptophyte, and a cryptophyte were identified, while primers specific for form IA/B RubisCO detected a diverse autotrophic community of chlorophytes, cyanobacteria, and chemoautotrophic proteobacteria. Form ID RubisCO dominated phytoplankton communities in both lobes of the lake and closely matched depth profiles for photosynthesis and chlorophyll. Our results indicate a coupling between light availability, photosynthesis, and *rbcL* mRNA levels in deep phytoplankton populations. Regulatory control of *rbcL* in phytoplankton living in nutrient-deprived shallow depths does not appear to be solely light dependent. The distinct water chemistries of the east and west lobes have resulted in depth- and lobe-dependent variability in RubisCO diversity, which plays a role in transcriptional activity of the key gene responsible for carbon fixation.

The McMurdo Dry Valleys form the largest ice-free region (~4,000 km^2) on the Antarctic continent (5). Owing to both the unique ecosystems they harbor and their sensitivity to environmental perturbation, the dry valleys are protected as an Antarctic Special Managed Area under environmental protection protocols of the Antarctic Treaty. Despite classification as a hyperarid cold desert (with an average temperature of ~−17°C and precipitation equivalent to <10 mm water), the dry valleys contain a mosaic of hydrologically closed lake basins that act as microbial oases, providing a year-round liquid water habitat for phototrophic, chemoautotrophic, and heterotrophic microorganisms that are isolated from direct contact with the atmosphere by permanent 3- to 6-m-thick ice covers (38). The perennial ice cover prevents wind-driven turbulence, allowing strong vertical stratification of both chemical and biological characteristics to exist in the water column. Although the ice attenuates more than 95% of incident light and narrows the solar spectrum to blue-green wavelengths, the liquid water columns of these lakes support primary producers, dominated by low-light-adapted phytoplankton, which provide fixed carbon for the strictly microbial food web (30, 40). Microscopic and pigment analyses of samples collected during the spring and summer showed that the phytoplankton communities are strongly vertically stratified within the water columns in response to gradients in light and nutrients. Maximum productivity occurs close to the chemocline (39).

Lake Bonney is one of several lakes in the Taylor Valley, Antarctica, which have been studied since 1993 as part of the McMurdo Long Term Ecological Research Program (http://www.mcmlter.org/). Dry valley lake aquatic systems support distinct microbial communities containing bacteria, algae, and flagellated and ciliated protozoans that interact to form truncated food webs dominated exclusively by microorganisms. Stratified phototrophic protist populations, including cryptophytes, chlorophytes, and chrysophytes, play key roles in primary productivity and carbon cycling in the lake food web (21, 27, 40). In one of the first phylogenetic studies conducted in Lake Bonney, Bielewicz et al. (2) characterized protist diversity through the stratified water columns of both lobes of Lake Bonney. The 18S rRNA libraries revealed that more than 85% of the sequences aligned with those of known phototrophic microbial eukaryotes. Shallow depths in the lake were dominated by a cryptophyte population related to *Geminigera cryophila*, mid-depths (13 to 15 m) harbored haptophytes and stramenopiles related to *Isochrysis* and *Nannochloropsis*, respectively, and the deepest photic zone was dominated by a variety of chlorophytes (2).

Ribulose-1,5-bisphosphate carboxylase/oxygenase (RubisCO) catalyzes the first step in CO_2 fixation. Four holoenzyme forms, I, II, III, and IV, are recognized in both phototrophic and chemotrophic organisms (47). Form I is the major CO_2 fixation enzyme found in plants, eukaryotic algae, cyanobacteria, and most phototrophic and chemolithoautotrophic proteobacteria (46). Most phytoplankton populations harbor one of four subclasses of form I RubisCO, including marine α-cyanobacteria (form IA), chlorophytes and β-cyanobacteria (form IB), and chromophytic algae such as diatoms and prymnesiophytes (form ID) (47). The

Received 4 January 2012 **Accepted** 28 March 2012
Published ahead of print 6 April 2012
Address correspondence to Rachael M. Morgan-Kiss, morganr2@muohio.edu.
This article is dedicated to the memory of John Hawes, Supervisor of the Center for Bioinformatics and Functional Genomics at Miami University.
Supplemental material for this article may be found at http://aem.asm.org/.
Copyright © 2012, American Society for Microbiology. All Rights Reserved.
doi:10.1128/AEM.00029-12

large subunit of RubisCO form I, encoded by the *rbcL* gene, is highly conserved and has been used as a phylogenetic tool in a variety of aquatic environments (e.g., see references 6, 11, and 15).

Logistical constraints have restricted most research in the McMurdo Dry Valleys to the austral spring, summer, and autumn months (10, 39), leaving us with little information on how the stratified microbial communities residing in the water columns of the lakes in this region respond to extended dark periods. We present data from the first study to examine responses of the dry valley lake autotrophic communities residing in Lake Bonney to the transition from full sunlight to the polar night. We focused specifically on the influence of the polar night transition on trends in primary production as well as on RubisCO dynamics through the photic zone.

MATERIALS AND METHODS

Site description. Lake Bonney lies immediately east of the Taylor Glacier, a major outlet glacier of the East Antarctic Ice Sheet. An ice-covered bedrock sill separates the lake into two basins, an east (ELB; 3.5 km^2) and a west (WLB; 1.3 km^2) lobe. The sill isolates saline, nutrient-rich deep waters while allowing the surface oxygenated waters (above 13 m in depth) to flow from WLB to ELB during the summer. The lake is fed at the west lobe by intermittent glacial meltwater at the terminus of the Taylor Glacier. An iron-rich subglacial brine pool called Blood Falls also flows seasonally into WLB (29). The lack of turbulent mixing leads to density-driven stratification of the water columns, producing stable gradients in temperature and conductivity. Approximately 1 to 5% of incident irradiance penetrates the ice cover, and the photic zones of both lobes extend from the bottom of the ice cover to the permanent nutricline (25). Both lobes exhibit unbalanced ratios of nitrogen to phosphorus: shallow phytoplankton populations are phosphorus limited (24, 39), while the phytoplankton residing near the chemocline depends upon upward nutrient diffusion from nutrient-rich deep waters (39). Lastly, long separation and differential evaporative histories between the two lobes have led to distinctive water chemistry differences in the isolated bottom waters. In the west lobe, oxygenated surface waters overlay anoxic layers with low nitrate and high ammonium levels, while the east lobe exhibits suboxic waters below the chemocline, with extremely high nitrate and nitrous oxide levels (50, 52).

Field sampling. Our study was conducted over one field season, from 17 February to 15 April 2008. A total of 28 water samples from ELB and 20 water samples from WLB were collected from late February to early April (sampling dates were 24 February, 2 March, 9 March, 16 March, 24 March, 29 March, and 10 April), a period representing the transition from 24 h of sunlight to complete darkness beneath the ice covers. Holes in the ice covers of the east and west lobes were drilled with a 10-cm-diameter ice auger and enlarged by melting with circulating heated ethylene glycol through a copper pipe. Sampling depths (6 m, 13 m, 18 m, and 20 m for ELB and 10 m, 13 m, 15 m, and 20 m for WLB) were measured from the piezometric water level in the ice hole (approximately 30 cm below the ice surface), using a depth-calibrated hand winch. Depths chosen coincided with chlorophyll *a* (Chl *a*) maxima reported in earlier studies (24) and spanned the photic zone (25). In addition, the locations of the Chl *a* maxima were confirmed on the day of sampling by performing a depth profile of Chl *a in situ*, using a bbe Moldaenke profiling spectrofluorometer (1). At each time point, lake water was collected from both lobes at each sampling depth, using a 5-liter Niskin bottle sampler (General Oceanics, FL), and 1 liter was concentrated onto sterile 47-mm, 0.45-μm-pore-size Durapore polyvinylidene fluoride membrane filters (Millipore, MA), using a vacuum of 0.3 atm. The filters were then frozen immediately in liquid nitrogen before being transported to McMurdo Station, where they were shipped on dry ice to U.S. laboratories and stored at −80°C until nucleic acid extraction.

Limnological variables. Conductivity, temperature, photosynthetically available radiation (PAR), light-mediated primary productivity (PPR), and Chl *a* were collected and measured using previously described methods (37). Briefly, temperature and conductivity were measured with a Seabird model 25 profiler as described by Spigel and Priscu (43). Depth profiles for *in situ* PAR were measured with a Li-Cor LI-193 spherical quantum sensor (Li-Cor Biosciences, NE). PAR levels were recorded manually at 0.5-m intervals from the piezometric water level to approximately 5 m below the photic zone (depth of 25 m). Levels of all inorganic nitrogen species were determined with a Lachat autoanalyzer, using methods described by Priscu (37). Owing to the low levels of soluble reactive phosphorus (SRP) in Lake Bonney, SRP was analyzed manually using the antimony-molybdate method (45) with a 10-cm-path-length cuvette. *In situ* Chl *a* was determined with a bbe Moldaenke profiling spectrofluorometer (1). This instrument was lowered at a rate that produced ~10 measurements m^{-1}, which was adequate to define the highly layered phytoplankton species. Vertical profiles of primary productivity were made by measuring [^{14}C]bicarbonate incorporation into particulate matter over a 24-h *in situ* incubation of 2 light bottles and 1 dark bottle at selected depths. The radioactivity in the dark bottles was subtracted from that in the light bottles to correct for nonphotosynthetic incorporation. Following incubation, samples were filtered onto Whatman GF/F filters, acidified with 0.5 ml 3 N HCl, air dried at 50°C, and counted using standard scintillation spectrometry. The concentration of dissolved inorganic carbon required for productivity rate calculations was determined by passing the gas from acid-sparged samples through a calibrated infrared gas analyzer. Depth-integrated estimates for PPR and Chl *a* in shallow (4 to 8 m), middle (10 to 15 m), and deep (18 to 20 m) populations residing within the photic zone were calculated as the sums of the measurements at sampling depths of 4 to 8 m, 10 to 15 m, and 18 to 20 m, respectively, according to the method of Lizotte et al. (27).

Nucleic acid isolation. Frozen filters were cut in half to allow for extraction of environmental RNA and DNA from the same filter. For environmental DNA, half of a filter was cut into small pieces and DNA was isolated using a FastDNA spin kit for soil (MP Biomedicals, OH) following the manufacturer's protocol. Total RNA was isolated from the other half of the filter by use of a combination of RNeasy miniprep (Qiagen, CA) and FastRNA Pro Soil-Direct (MP Biomedicals, OH) kits (see the supplemental material for more details), according to the method of Kong and Nakatsu (17). For reverse transcription, total RNA ranging from 5 to 30 ng was reverse transcribed to single-stranded cDNA by use of an iScript cDNA synthesis kit (Bio-Rad, CA) as specified by the manufacturer. Negative controls (replacing RNA with water in the reaction mixture) were included in all experiments.

Real-time qPCR. Quantification of the RubisCO gene copy number and transcript level was performed using real-time quantitative PCR (qPCR) with primer sets that target different forms of RubisCO genes (see the supplemental material for more details). The primer sets targeting form IA/B and form ID RubisCO genes were developed as previously described (33). Form ID and IA/B RubisCO clades represent the dominant isoforms in marine and freshwater systems (33, 35, 54). The primer set GemF2 plus GemR2 was designed for this study to target the cryptophyte *Geminigera cryophila*, possessing the form ID RubisCO gene. This organism was previously found in 18S rRNA clone libraries (2) but could not be detected in this study by use of the form ID primer set. The species-specific primer set GemF2 plus GemR2 (GemF2, GCGTTTCTTATTCG GTATGGA; and GemR2, GGCCACAGTGAATACCACCT) was designed using the program Primer3, based on the *rbcL* sequence of *G. cryophila* (GenBank accession no. AB164411).

qPCR was performed according to a previously described method (2), using a 25-μl reaction mixture containing 1 μl of cDNA or DNA (10 ng), 1.5 μl of each primer (10 pmol μl^{-1}), and 12.5 μl iQ SYBR green Supermix (Bio-Rad, CA). Amplification conditions were 5 min at 95°C followed by 35 cycles of 1 min at 94°C, 20 s at 52°C, and 30 s at 72°C, and fluorescence intensity was acquired at 83°C (above the melting point of primer dimers). To determine the melting temperature and PCR product specificity, a melting curve was acquired by heating from 50°C to 95°C. Data

analysis was carried out using iCycler iQ optical system software, version 3.01 (Bio-Rad, CA). The threshold cycle (C_T) was defined as the cycle number at which a statistically significant increase in fluorescence was detected. The detection limit for qPCR was 100 copies liter^{-1}, and the amplification efficiency was >85%.

Clone library construction and sequencing. For simplicity, all RubisCO large-subunit genes identified in this paper are referred to as *rbcL*. Gene fragments were amplified from DNA or cDNA by use of form ID and IA/B primer sets to generate PCR products for cloning. PCR was performed in triplicate, using 25 cycles of 94°C for 1 min, 52°C for 20 s, and 72°C for 30 s. Gel-purified PCR products were ligated into the pGEM-T Easy vector (Promega, WI) and transformed into TOP10 cells. A total of 27 DNA- and cDNA-based clone libraries were generated for selected environmental samples from various time points and depths within each lobe (see Table S1 in the supplemental material for sample locations and dates). Plasmid DNAs (30 per library) containing unique inserts were used as templates for PCR with the M13 vector primer set. Sequencing reactions were performed using a BigDye Terminator v3.1 cycle sequencing kit (Applied Biosystems, CA) with the M13R primer, and the fragments were sequenced on an ABI model 3730xl DNA analyzer (Applied Biosystems, CA). Multiple alignments among the current sequences were performed using CLUSTALW in MEGA 5. Sequences with >90% nucleotide similarity were grouped into the same operational taxonomic unit (OTU). BLASTn (www.ncbi.nlm.nih.gov/BLAST/) was used to search GenBank for nearest relative sequences to OTUs. The current OTUs and nearest relative sequences from GenBank were aligned by using CLUSTALW in MEGA 5. Phylogenetic trees were constructed by the neighbor-joining method with a Kimura two-parameter distance model, using MEGA 5 software. Bootstrapping was used to estimate the reliability of phylogenetic trees, with 1,000 replicate trees.

Statistical analysis. Graphic figures were generated in SigmaPlot 9.0 (Systat Software, Inc., CA) and OriginPro 8.5.1 (OriginLab Corp., Northampton, MA). Relationships between PAR and PPR, Chl *a*, *rbcL* copy number, or *rbcL* transcript abundance were determined using Pearson correlation (*R*) analysis (40a). All data were log transformed prior to analysis. PPR data represent the means for two independent samples. qPCR data represent the means for four replicates measured from one environmental sample.

Nucleotide sequence accession numbers. Sequences generated in this study have been deposited in the National Center for Biotechnology Information GenBank database under accession numbers GU132860 to GU132939.

RESULTS

General lake characteristics. Physical and chemical profiles in Lake Bonney revealed a highly stratified vertical structure of the water column within each lobe (Fig. 1). The water temperature reached a maximum in the middle of the water column and ranged from −2.1 to 4.9°C in ELB and from −4.3 to 2.2°C in WLB (Fig. 1A). ELB and WLB both have steep mid-depth conductivity gradients, with values ranging from 0.36 to 109.13 mS cm^{-1} and from 0.74 to 79.60 mS cm^{-1}, respectively (Fig. 1B). Both lobes showed distinct light-dependent PPR and Chl *a* maxima at 13.5 m, or just above the chemocline (Fig. 1C and D). Maximum PPR was 4- to 5-fold higher in ELB (Fig. 1C), while the Chl *a* maximum was 2-fold higher in WLB than in ELB (Fig. 1D).

Effect of polar night transition on photosynthesis and phytoplankton biomass. We monitored responses of the phototrophic community through the photic zone during the summer-winter transition. Beginning in mid-February, daily under-ice irradiance declined rapidly in both lobes of Lake Bonney (Fig. 2A and B). Depth-integrated Chl *a* concentrations and photosynthetic rates were calculated for the three major phytoplankton assemblages, i.e., shallow, mid-depth, and deep populations.

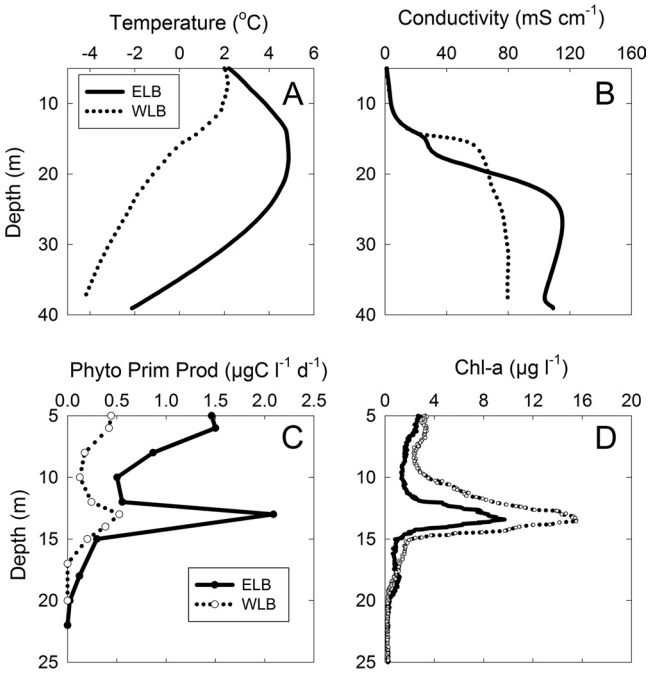

FIG 1 Water column characteristics of the east (ELB) and west (WLB) lobes of Lake Bonney. All depths are from the piezometric water level within the sampling hole. The ice cover was ~3.5 m thick. Sampling dates were as follows: for ELB, 12 March 2008 (all measurements); and for WLB, 15 March 2008 (PPR) and 16 March 2008 (temperature, conductivity, and Chl *a*).

Phytoplankton residing in the shallow and mid-depths responded to the decline in PAR during the summer-winter transition by a reduction in PPR (Fig. 2C to F). Photosynthetic rates in the deepest layer were very low in both lobes throughout the sampling period. Deep populations in ELB exhibited a rapid decline in PPR in early January, while WLB deep populations exhibited low photosynthetic rates throughout the polar night transition (Fig. 2G and H). In contrast with phytoplankton photosynthesis, Chl *a* levels generally increased during the summer-winter transition (Fig. 2C to F). However, while shallow populations exhibited a steady rise in Chl *a* levels throughout the sampling period, Chl *a* stabilized at mid-depths by mid-March (Fig. 2E and F) and exhibited a decline in deep populations beginning in mid-February (Fig. 2G and H). To determine whether PPR or Chl *a* covaried with declining PAR, Pearson correlation coefficients were determined at four sampling depths throughout the photic zone between sampling dates 24 February and 10 April (Table 1). Depths at or above the chemocline (i.e., 6 m and 13 m in ELB and 10 m and 13 m in WLB) exhibited a positive correlation between PPR and PAR in both lobes ($r = 0.82$ to 0.99; $P < 0.05$) (Table 1) during the polar night transition. In contrast to the case for photosynthetic rates, shallow populations from both lobes exhibited a negative correlation between PAR and Chl *a* ($r = -0.792$; $P < 0.1$) (Table 1).

RubisCO diversity. To gain a better understanding of autotrophic gene diversity in Lake Bonney, clone libraries were generated for the RubisCO large-subunit gene, using DNA and mRNA (reverse transcribed to cDNA) as templates. A total of 4 phylotypes were detected in the form ID DNA and cDNA clone libraries (Fig. 3). The vast majority of form ID *rbcL* sequences were

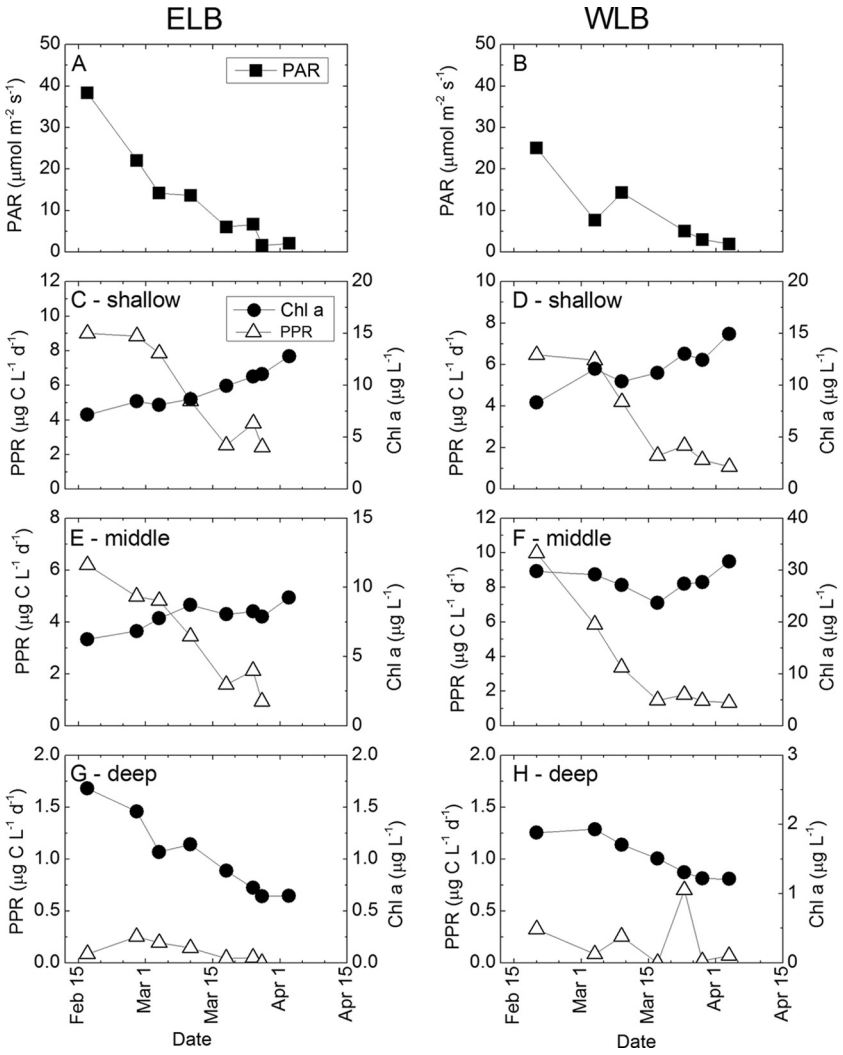

FIG 2 Temporal changes during the summer-winter transition in photosynthetically active radiation immediately beneath the ice (A and B) and in chlorophyll *a* concentration and photosynthetic rate (C to H), integrated for shallow (4 to 8 m) (C and D), middle (10 to 15 m) (E and F), and deep (18 to 20 m) (G and H) phytoplankton populations residing in the photic zone of Lake Bonney. PAR was measured at a depth of 10 m. PAR, photosynthetically active radiation; PPR, photosynthetic rate; Chl *a*, chlorophyll *a* concentration. Note that different scales for Chl *a* and PPR are used for each vertically distinct population.

related to a stramenopile, *Nannochloropsis* (GenBank accession no. DQ977734; 97% similarity), and a haptophyte, *Isochrysis* sp. (GenBank accession no. AB043693 and AY119783; 91% similarity). Using cryptophyte-specific *rbcL* primers, we also detected a single cryptophyte, which was related to *Geminigera cryophila* (GenBank accession no. AB164411; 99% similarity). The dominant form ID phylotypes were detected in both lobes of Lake Bonney and were present in both DNA and cDNA libraries; however, haptophyte sequences dominated cDNA libraries in both lobes (Fig. 3; also see Fig. S1 in the supplemental material).

A total of 15 phylotypes were detected in the form IA/B DNA and cDNA clone libraries, related to cyanobacteria, chlorophytes, and chemoautotrophic proteobacteria (see Fig. S2 to S4 in the supplemental material). More than 95% of cyanobacterial sequences were found in the DNA clone libraries only and were related to *Nostocales* and *Oscillatoriales* (see Fig. S2 in the supplemental material). *Nostocales* sequences were restricted to WLB, while *Oscillatoriales* sequences were detected throughout the water columns of both lobes. While cyanobacterial *rbcL* genes were rare in the cDNA clone libraries, chlorophyte *rbcL* genes related to those in *Micractinium* and *Chlorella* spp. (GenBank accession no. EF113451 and AB260909; 94% similarity), as well as the Antarctic chlorophytes *Chloromonas* and *Chlamydomonas* spp. (GenBank accession no. U80809 and AY731086; 90 and 99% similarity, respectively), dominated form IA/B RubisCO cDNA clone libraries (see Fig. S3 and S5 in the supplemental material). Lastly, form IA/B sequences related to chemoautotrophic proteobacteria (an endosymbiont of *Oligobrachia haakonmosbi* and *Thiobacillus* [GenBank accession no. AB057772 and AY914807; 83 and 87% similarity, respectively]) were recovered from DNA libraries from WLB samples located below the chemocline. No chemoautotroph sequences were recovered from ELB clone libraries (see Fig. S4 and S5 in the supplemental material).

Depth- and lobe-specific RubisCO trends. Given the current lack of data on abundance or expression levels of autotrophic genes in dry valley environments, we used qPCR to measure ver-

TABLE 1 Polar night transition-dependent Pearson correlations for PPR, Chl *a*, *rbcL* gene copy number (DNA), and *rbcL* transcript level (mRNA) versus PAR[a]

	Pearson correlation coefficient (*R*)					
			rbcL DNA		*rbcL* mRNA	
Sampling depth (m)	PPR	Chl *a*	Form ID	Form IA/B	Form ID	Form IA/B
ELB sampling depths						
6	0.934**	−0.792*	−0.219	−0.797*	−0.150	0.070
13	0.948**	−0.276	0.808*	−0.375	0.754*	0.854**
18	0.994**	0.386	0.815*	0.843**	0.554	0.737*
20	0.673	0.939*	0.604	0.586	0.731	−0.700
WLB sampling depths						
10	0.860*	−0.792*	0.468	0.517	0.339	−0.575
13	0.862*	−0.276	−0.313	−0.982**	0.212	−0.860
15	0.338	0.354	0.551	−0.437	0.148	−0.600
20	−0.922*	0.916**	−0.610	−0.809	−0.030	−0.038

[a] Samples were collected between 24 February and 10 April 2008. All data were log transformed prior to analysis. Sampling depths were measured from the piezometric water level within the sampling hole. *, significant correlation ($P < 0.1$); **, significant correlation ($P < 0.05$).

tical trends in RubisCO gene copy number (DNA) versus gene expression (mRNA) within the photic zones (≤20 m) of both lobes of Lake Bonney (Fig. 4). Form ID RubisCO was numerically dominant at the levels of gene copy number (DNA) and gene expression (mRNA) in both lobes. Furthermore, vertical trends in form ID DNA and mRNA resembled those for PPR and Chl *a* (Fig. 1C and D and 4A and C). In comparison with form ID RubisCO abundance, levels of form IA/B RubisCO were reduced by as much as 1,600- and 6,000-fold for DNA and mRNA, respectively, with the largest differences occurring at mid-depth (13 m) in WLB (Fig. 4). Furthermore, vertical trends in both form IA/B RubisCO gene copy and transcript levels were distinct from those for form ID RubisCO. In ELB, form IA/B DNA and mRNA peaked in the near-surface waters and declined up to 100-fold in deeper populations. In contrast, in WLB, form IA/B DNA was relatively constant and form IA/B mRNA remained low ($<10^3$ copies liter^{-1}) throughout the photic zone (Fig. 4B and D).

Transcriptional activity (i.e., the ratio of mRNA to DNA) in Lake Bonney was very low ($\ll 1$), and vertical trends in transcriptional activity were unique for each lobe (Fig. 4E and F). In ELB, the form ID mRNA/DNA ratio increased with lake depth, while form IA/B transcriptional activity declined 8-fold at deep versus shallow sampling depths (Fig. 4E and F). RubisCO transcriptional activity was very low in the west lobe compared to that in the east lobe. Ratios of mRNA to DNA were as much as 25- and 593-fold lower for forms ID and IA/B, respectively, for WLB than for ELB (Fig. 4E and F).

RubisCO dynamics during the polar night. Seasonal dynamics of RubisCO during the polar night transition were determined throughout the photic zones of both lobes of Lake Bonney (Fig. 5). Form ID RubisCO dominated the autotrophic communities of both lobes throughout the summer-winter transition, at the levels of both transcript abundance and copy number. In ELB, the abundances of form ID mRNA and DNA in samples from 13 m, as well as form ID DNA in samples from 18 m, declined during the polar night (Fig. 5A and C) and were positively correlated with PAR ($r =$ 0.81 to 8.85; $P < 0.1$) (Table 1). In contrast, samples from both 13 m and 15 m from WLB exhibited an initial 7-fold decline in form ID mRNA abundance, followed by a 3- to 5-fold increase in form ID mRNA levels at a later (8 March) sampling time (Fig. 5E and G). No positive correlation ($P > 0.1$) between form ID mRNA and PAR was observed in samples collected from WLB (Table 1). Haptophyte sequences dominated the cDNA clone libraries at mid-depth (13 m) for both lobes at early (24 February) and late (29 March) time points (see Fig. S1 in the supplemental material). In contrast to the case for samples from 13 m, haptophytes replaced stramenopiles during the summer-winter transition at a shallow (6 m) depth in ELB, while the opposite trend was observed for a shallow (10 m) depth in WLB (see Fig. S1 in the supplemental material).

Form IA/B mRNA and DNA levels exhibited trends that were both depth and lobe dependent. In ELB, form IA/B exhibited a positive correlation between PAR levels and mRNA abundance at 13 m and both mRNA and DNA abundances in 18-m populations ($r =$ 0.74 to 0.85; $P < 0.1$) (Fig. 5B and D; Table 1). However, samples from 6 m exhibited a 7-fold rise in form IA/B DNA during the polar night transition, as well as a negative correlation with PAR ($r =$ −0.80; $P < 0.1$) (Table 1). Form IA/B mRNA and DNA levels were generally lower in the west lobe (Fig. 5F and H). Furthermore, no significant trends between form IA/B abundance and PAR levels were observed in WLB, and form IA/B mRNA and DNA levels increased in most sampling depths by 1.6- to 3.9-fold during the polar night transition (Table 1; Fig. 5F and H). Form IA/B DNA clone libraries (generated from samples taken on 2 March) revealed a mixed population of cyanobacteria, chlorophytes, and chemotrophs in WLB. However, ELB form IA/B clone libraries harbored a less diverse population of cyanobacteria and chlorophytes, and form IA/B cDNA libraries from ELB were dominated almost exclusively by chlorophyte mRNAs (see Fig. S5 in the supplemental material).

DISCUSSION

Permanently ice-covered Antarctic lakes harbor few metazoans, do not mix seasonally, have low allochthonous input, and are exposed to minimal direct human impact. As such, the vast majority of the organic carbon that supports this ecosystem is provided by carbon fixation by autotrophic microorganisms. Past studies have shown that phytoplankton productivity in the short austral summer is limited by under-ice PAR levels (10, 12, 23) as well as by nutrient availability (39). Our study extends this earlier work and shows that Lake Bonney phytoplankton populations exhibit distinct seasonal and spatial trends in photosynthesis and RubisCO gene dynamics.

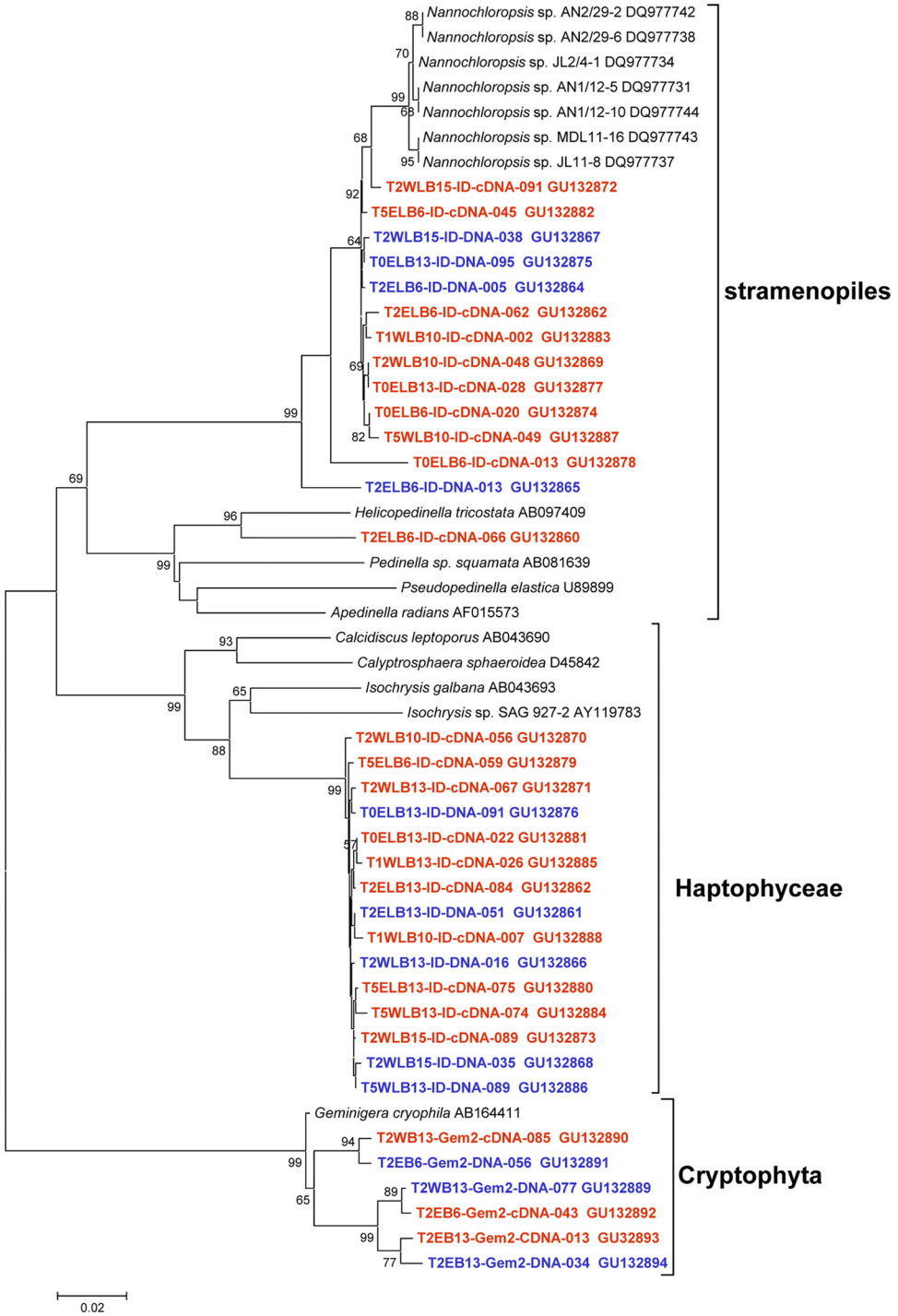

FIG 3 Neighbor-joining phylogenetic tree of representative form ID *rbcL* sequences (615 bp) retrieved from environmental DNA (blue) and mRNA (red) from Lake Bonney. Bar, 0.02 substitution per nucleotide position. The GenBank accession number is listed after each sequence name. Clones were named as follows: time point with lake name and depth-primer name-template type-index number.

In high-latitude aquatic habitats such as dry valley lakes, seasonal transitions during winter-spring and autumn-winter are accompanied by extreme changes in day length and incident irradiance. Phytoplankton residing in either lobe of Lake Bonney responded to the seasonal loss in PAR during the summer-winter transition by an overall reduction in photosynthesis throughout the photic zone. This trend was most pronounced in middle and deep populations, which experienced lower PAR levels earlier in the summer-winter transition than those of phytoplankton residing in the shallow layers (Fig. 2). Conversely, Chl *a* in the shallow populations increased throughout our sampling period, while Chl *a* in the deeper populations remained unchanged (mid-depths) or

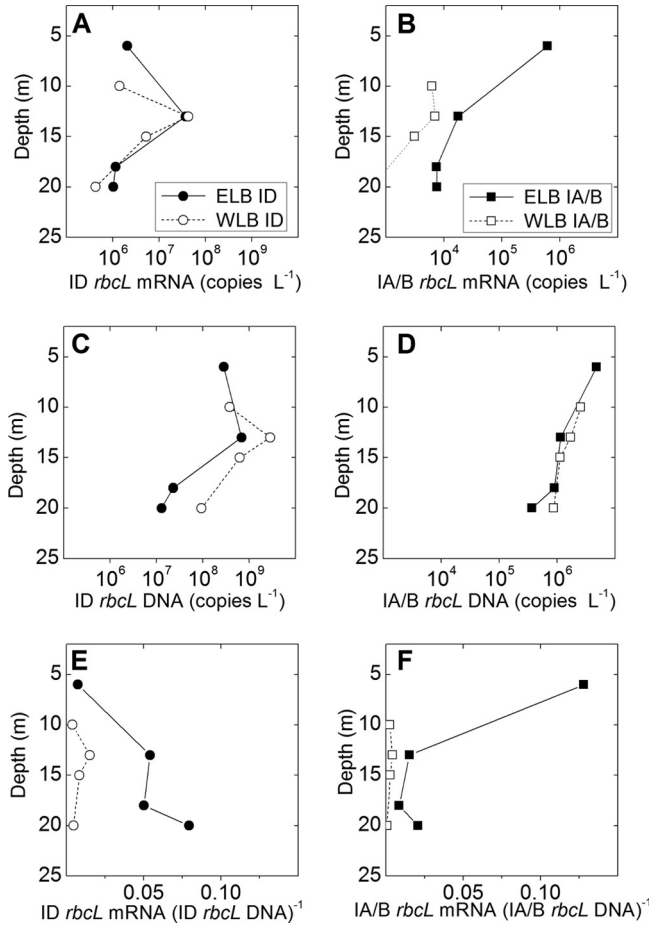

FIG 4 Effect of lake depth on *rbcL* abundance at the levels of transcript abundance (A and B), gene copy number (C and D), and ratio of mRNA to DNA (E and F). Abundance was quantified for RubisCO isoforms ID (A, C, and E) and IA/B (B, D, and F) by using qPCR. Water samples were collected on 9 March. Note that data in panels A to D are presented on log scales. Data points represent the means for four replicates from one sample.

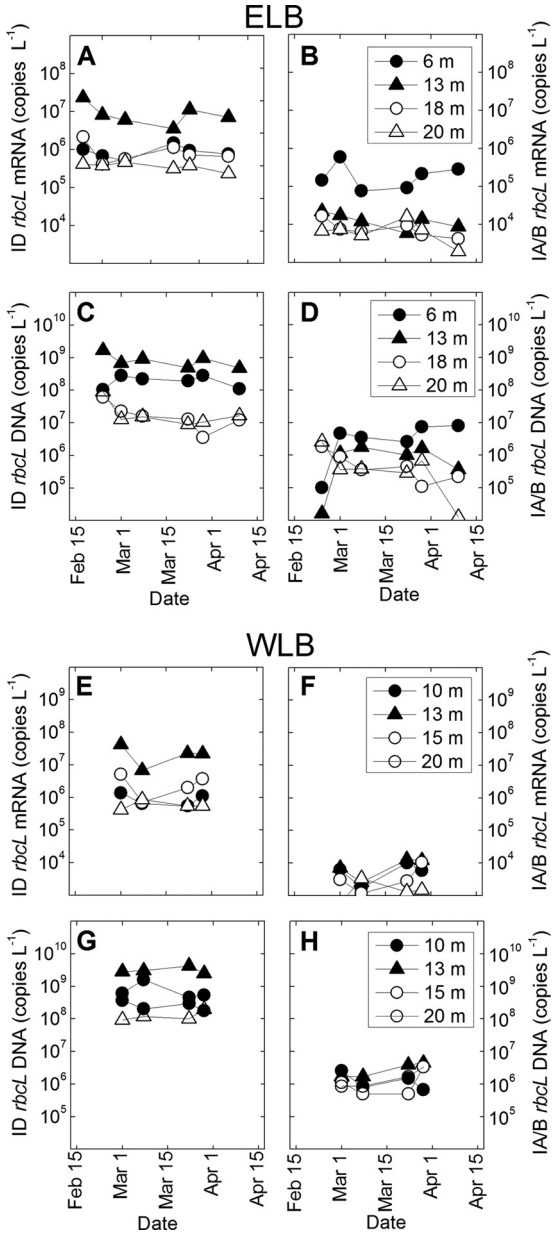

FIG 5 Temporal changes in *rbcL* transcript abundance and gene copy number measured in Lake Bonney during the summer-winter transition. Dynamics of form ID *rbcL* (A, C, E, and G) and IA/B *rbcL* (B, D, F, and H) were monitored via qPCR at four sampling depths in ELB and WLB during the polar night between 24 February and 10 April. Data points represent the means for four replicates from one sample.

declined (deep layer). These data show that sustained light-dependent CO_2 fixation in shallow and middle populations supported phytoplankton biomass accumulation later into the summer-winter transition than that of the deep chlorophyll layer in both lobes of Lake Bonney. Similarly, during the early spring, phytoplankton biomass develops sequentially from the shallow to the deep layers of the photic zone in response to the seasonal increase in PAR (27).

While a recent study provided molecular evidence for vertical stratification and seasonal variability in the Lake Bonney protist community (2), little is known of the relative contributions of specific phytoplankton groups to primary productivity in the dry valley lake food web. In agreement with previous reports (2, 19, 26, 41), our functional analyses of a key photosynthetic gene confirmed that a stratified autotrophic community dominated by photosynthetically active protists occupies the photic zone of Lake Bonney. First, a population of stramenopiles related to *Nannochloropsis* was abundant throughout the water columns of both lobes. Results from cDNA clone libraries from this study indicate that *Nannochloropsis* is an active member of the primary producer population (see Fig. S1 in the supplemental material). *Nannochloropsis*-dominated algal blooms have been detected in other aquatic systems during cold-water periods (7, 8, 18), implying that they are adapted to low temperatures. Second, a cryptophyte species identified as *Geminigera cryophila* was identified as an active member in the shallow layers (see Fig. S6 in the supplemental material). Finally, a haptophyte related to an *Isochrysis* sp. made up 95 to 100% of sequences recovered from cDNA libraries generated from 13-m samples for both lobes (see Fig. S1 in the supplemental material). *Isochrysis* populations also occur at the same depth as high concentrations of dimethylsulfide in Lake Bonney, and they may produce biogenic sulfur compounds as cryoprotectants (20).

While regulation of RubisCO enzyme activity is complex, most phototrophic organisms actively transcribe the gene encoding the large subunit, and the *rbcL* gene copy number, transcript abundance, and phylogenetic diversity have been applied as molecular indicators of carbon fixation potential in aquatic environments (13–15, 28, 32, 53, 54). Photoautotrophs harboring form ID RubisCO dominate the photic zone of Lake Bonney, with maximum transcript levels and gene copy numbers occurring at mid-depth (13 m) in both lobes. Vertical trends in form ID abundance matched those of PPR and phytoplankton biomass (this study), as well as 18S rRNA transcript abundance (2), suggesting that phytoplankton populations harboring form ID RubisCO are key primary producers in the dry valley lake food web. Phytoplankton populations residing in Lake Bonney balance light availability with a sufficient supply of nutrients by residing at depths directly above the chemocline (22, 27, 39). Furthermore, we observed a strong correlation between declining PAR and both form ID gene copy number and mRNA level in this phytoplankton population (Table 1). Taken together, these data imply that at the depth of maximum productivity, there is a coupling between PAR, photosynthetic rates, and transcriptional activity of the major isoform of RubisCO.

While phytoplankton populations residing in Lake Bonney are always light limited (24), productivity in the surface waters is under extreme nutrient deprivation for most of the austral summer (39). Nutrient deficiency develops under the ice in early spring and persists throughout the summer, until either nutrient pools are recharged in the winter or a transient influx of glacial meltwater introduces glacial flour particles to the water column (25). In support of earlier reports that observed lower photosynthetic productivity and photosynthetic efficiency within surface layers of Lake Bonney (22, 27, 39), *rbcL* DNA and mRNA levels measured in shallow samples from either lobe were >100-fold lower than those of mid-depth populations (Fig. 4). Despite a strong relationship between light availability and photosynthetic rates in surface populations, no positive correlation was observed between PAR and RubisCO abundance in the shallow layers of Lake Bonney (Table 1). This lack of a relationship between PAR and RubisCO suggests that additional factors are likely to influence *rbcL* activity in the phytoplankton residing in the shallow layers of Lake Bonney. A recent study on diel responses in natural phytoplankton populations from the Mississippi and Orinoco River plumes found that daily patterns of *rbcL* transcript abundance were not only influenced by the diurnal light cycle but also impacted by nutrient deficiency (13). We suggest that nutrient deficiency may have played a role in the differential seasonal patterns in *rbcL* expression observed between the shallow and deeper phytoplankton populations. Nutrient stress may also influence coupling between RubisCO transcription and carbon fixation capacity in the shallow populations, which has been observed in other nutrient-deficient environments (13).

It should be noted that RubisCO is regulated not only transcriptionally but also at the level of enzyme activity (31). Studies have suggested that dissipation of excess energy products via photorespiration is an environmental stress response to nutrient deficiency in some phytoplankton communities (13, 16). Thus, regulation of enzyme activity could also influence carbon fixation rates during the polar night transition, particularly in nutrient-stressed shallow populations. Furthermore, while the application of qPCR to environmental samples has been adopted widely as a proxy for estimating the distribution and activity of microbial populations (e.g., see references 4, 9, 32, 44, and 49), there are caveats that should be considered in applying qPCR approaches to environmental samples. These considerations include variability in gene copy and genome numbers between organisms, as well as differences in nucleic acid extraction efficiencies and mRNA stability (reviewed in reference 42).

Both lobes of Lake Bonney support distinct subsets of metabolically active autotrophic communities that carry either form ID or IA/B RubisCO. The strong relationship between PAR, rates of primary production, and transcript levels of form ID RubisCO indicates that transcriptional regulation of this RubisCO isoform could be important for controlling rates of autotrophic carbon fixation. However, variability in vertical and temporal trends for both isoforms within and between the lobes suggests that light availability is not the sole factor influencing RubisCO dynamics in Lake Bonney autotrophic populations. Studies on other aquatic systems have shown that phytoplankton community composition contributes to (i) light-dependent patterns in *rbcL* transcript levels (13, 15, 34), (ii) the coupling between RubisCO gene expression and rates of photosynthesis (13), and (iii) the coupling between RubisCO activity and carbon fixation potential (16). Differences in autotrophic community structure and activity in the two lobes presumably reflect the climate evolution of the two lobes of the lake. Using helium isotope data, Poreda et al. (36) showed that these lake basins were isolated and possibly ice-free for thousands of years, until a major climate shift led to an overflow of water from the west lobe to the east lobe (43). This climate shift produced an important tipping point in the lake ecosystem, in terms of the development of a permanent ice cover and mixing of near-surface waters between the lobes. As a result of this evolution in physical and chemical character, biodiversity would have been altered significantly, culminating in the vertical structure that we observed in our present study. As such, climate must have played a key role in the differences in RubisCO diversity and regulation measured in our study. As the climate of Antarctica warms (51), we can expect to see new tipping points that may lead to further changes in dry valley lake food web structure. Thus, while the transition to polar night represents one of the most extreme seasonal changes experienced by the autotrophic organisms in Lake Bonney, the legacy of evolution of lake chemistry over the past 6,000 years may exert long-term selection pressures on the autotrophic biology of Lake Bonney, and presumably other lakes within the McMurdo Dry Valleys.

ACKNOWLEDGMENTS

We thank A. Chiuchiolo, E. Bell, E. Bottos, M. Lizotte, and the McMurdo LTER limnology team for collection and preservation of the samples in Antarctica. We thank Ratheon Polar Services and PHI helicopters for logistical support.

This work was supported in part by NSF Office of Polar Programs and Molecular and Cellular Biosciences grants 0631659 and 1056396 to R.M.M.-K. and 0631494, 432595, OPP 1115245, and 0237335 to J.C.P.

REFERENCES

1. **Beutler M, et al.** 2002. A fluorometric method for the differentiation of algal populations *in vivo* and *in situ*. Photosynth. Res. **72**:39–53.
2. **Bielewicz S, et al.** 2011. Protist diversity in a permanently ice-covered Antarctic lake during the polar night transition. ISME J. **5**:1559–1564.
3. Reference deleted.
4. **Church MJ, Short CM, Jenkins BD, Karl DM, Zehr JP.** 2005. Temporal patterns of nitrogenase gene (*nifH*) expression in the oligotrophic North Pacific Ocean. Appl. Environ. Microbiol. **71**:5362–5370.
5. **Doran PT, et al.** 2002. Antarctic climate cooling and terrestrial ecosystem response. Nature **415**:517–520.

6. **Elsaied HE, Kimura H, Naganuma T.** 2007. Composition of archaeal, bacterial, and eukaryal RubisCO genotypes in three Western Pacific arc hydrothermal vent systems. Extremophiles **11**:191–202.
7. **Fawley KP, Fawley MW.** 2007. Observations on the diversity and ecology of freshwater *Nannochloropsis* (Eustigmatophyceae), with descriptions of new taxa. Protist **158**:325–336.
8. **Fietz A, et al.** 2005. First record of *Nannochloropsis limnetica* (Eustigmatophyceae) in the autotrophic picoplankton from Lake Baikal. J. Phycol. **35**:780–790.
9. **Freitag TE, Prosser JI.** 2009. Correlation of methane production and functional gene transcriptional activity in a peat soil. Appl. Environ. Microbiol. **75**:6679–6687.
10. **Fritsen CH, Priscu JC.** 1999. Seasonal change in the optical properties of the permanent ice cover on Lake Bonney, Antarctica: consequences for lake productivity and dynamics. Limnol. Oceanogr. **44**:447–454.
11. **Giri BJ, Bano N, Hollibaugh JT.** 2004. Distribution of RubisCO genotypes along a redox gradient in Mono Lake, California. Appl. Environ. Microbiol. **70**:3443–3448.
12. **Herbei R, et al.** 2010. Physiochemical properties influencing biomass abundance and primary production in Lake Hoare, Antarctica. Ecol. Model. **221**:1184–1193.
13. **John D, et al.** 2011. A day in the life in the dynamic marine environment: how nutrients shape diel patterns of phytoplankton photosynthesis and carbon fixation gene expression in the Mississippi and Orinoco River plumes. Hydrobiology **679**:155–173.
14. **John DE, Patterson SS, Paul JH.** 2007. Phytoplankton-group specific quantitative polymerase chain reaction assays for RubisCO mRNA transcripts in seawater. Mar. Biotechnol. **9**:747–759.
15. **John DE, et al.** 2007. Phytoplankton carbon fixation gene (RubisCO) transcripts and air-sea CO_2 flux in the Mississippi River plume. ISME J. **1**:517–531.
16. **Kana TM, Watts JL, Glibert PM.** 1985. Diel periodicity in the photosynthetic capacity of coastal and offshore phytoplankton assemblages. Mar. Ecol. Prog. Ser. **25**:131–139.
17. **Kong W, Nakatsu CH.** 2010. Optimization of RNA extraction for PCR quantification of aromatic compound degradation genes. Appl. Environ. Microbiol. **76**:1282–1284.
18. **Krienitz L, Hepperle D, Stich HB, Weiler W.** 2000. *Nannochloropsis limnetica* (Eustigmatophyceae), a new species of picoplankton from freshwater. Phycologia **35**:219–227.
19. **Lee PA, et al.** 2004. Thermodynamic constraints on microbially mediated processes in lakes of the McMurdo Dry Valleys, Antarctica. Geomicrobiol. J. **21**:1–17.
20. **Lee PA, et al.** 2004. Elevated levels of dimethylated-sulfur compounds in Lake Bonney, a poorly ventilated Antarctic lake. Limnol. Oceanogr. **49**:1044–1055.
21. **Lizotte MP, Priscu JC.** 1998. Distribution, succession and fate of phytoplankton in the dry valley lakes of Antarctica, based on pigment analysis, p 229–240. *In* Priscu JC (ed), Ecosystem dynamics in a polar desert: the McMurdo Dry Valleys, Antarctica. Antarctic Research Series, vol 72. American Geophysical Union, Washington, DC.
22. **Lizotte MP, Priscu JC.** 1994. Natural fluorescence and quantum yields in vertically stationary phytoplankton from perennially ice-covered lakes. Limnol. Oceanogr. **39**:1399–1410.
23. **Lizotte MP, Priscu JC.** 1990. Photosynthesis-irradiance relationships in phytoplankton from Lake Bonney. Antarct. J. U.S. **25**:223–224.
24. **Lizotte MP, Priscu JC.** 1992. Photosynthesis-irradiance relationships in phytoplankton from the physically stable water column of a perennially ice-covered lake (Lake Bonney, Antarctica). J. Phycol. **28**:179–185.
25. **Lizotte MP, Priscu JC.** 1992. Spectral irradiance and bio-optical properties in perennially ice-covered lakes of the dry valleys (McMurdo Sound, Antarctica). Antarct. Res. Ser. **57**:1–14.
26. **Lizotte MP, Priscu JP.** 1992. Algal pigments as markers for stratified phytoplankton populations in Lake Bonney (dry valleys). Antarct. J. U.S. **27**:259–260.
27. **Lizotte MP, Sharp TR, Priscu J.** 1996. Phytoplankton dynamics in the stratified water column of Lake Bonney, Antarctica. I. Biomass and productivity during the winter-spring transition. Polar Biol. **16**:155–162.
28. **Meakin NG, Wyman M.** 2011. Rapid shifts in picoeukaryote community structure in response to ocean acidification. ISME J. **5**:1397–1405.
29. **Mikucki JA, et al.** 2009. A contemporary microbially maintained subglacial ferrous "ocean." Science **324**:397–400.
30. **Morgan-Kiss RM, Priscu JP, Pocock T, Gudynaite-Savitch L, Hüner NPA.** 2006. Adaptation and acclimation of photosynthetic microorganisms to permanently cold environments. Microbiol. Mol. Biol. Rev. **70**:222–252.
31. **Ogren WL.** 2003. Affixing the O to Rubisco: discovering the source of photorespiratory glycolate and its regulation. Photosynth. Res. **76**:53–63.
32. **Paerl RW, Turk KA, Beinart RA, Chavez FP, Zehr JP.** 2012. Seasonal change in the abundance of *Synechococcus* and multiple distinct phylotypes in Monterey Bay determined by *rbcL* and *narB* quantitative PCR. Environ. Microbiol. **14**:580–593.
33. **Paul JH, Alfreider A, Wawrik B.** 2000. Micro and macrodiversity in *rbcL* sequences in ambient phytoplankton populations from the Southeastern Gulf of Mexico. Mar. Ecol. Prog. Ser. **198**:9–18.
34. **Paul JH, Kang JB, Tabita FR.** 2000. Diel patterns of regulation of *rbcL* transcription in a cyanobacterium and a prymnesiophyte. Mar. Biotechnol. **2**:429–436.
35. **Pichard SL, Campbell L, Paul JH.** 1997. Diversity of the ribulose bisphosphate carboxylase/oxygenase form I gene (*rbcL*) in natural phytoplankton communities. Appl. Environ. Microbiol. **63**:3600–3606.
36. **Poreda RJ, Hunt AG, Lyons WB, Welch KA.** 2004. The helium isotopic chemistry of Lake Bonney, Taylor Valley, Antarctica: timing of Late Holocene climate change in Antarctica. Aquat. Geochem. **10**:353–371.
37. **Priscu JC.** 1997. The biogeochemistry of nitrous oxide in permanently ice-covered lakes of the McMurdo Dry Valleys, Antarctica. Global Change Biol. **3**:301–305.
38. **Priscu JC.** 1998. Ecosystem dynamics in a polar desert: the McMurdo Dry Valleys, Antarctica. Antarctic Research Series, vol 72. American Geophysical Union, Washington, DC.
39. **Priscu JC.** 1995. Phytoplankton nutrient deficiency in lakes of the McMurdo Dry Valleys, Antarctica. Freshw. Biol. **34**:215–227.
40. **Priscu JC, et al.** 1999. Carbon transformations in a perennially ice-covered Antarctic lake. Bioscience **49**:997–1008.

40a. **R Development Core Team.** 2008. R: a language and environment for statistical computing. R Foundation for Statistical Computing, Vienna, Austria.

41. **Roberts EC, Priscu JC, Wolf CF, Lyons WB, Laybourn-Parry J.** 2004. The distribution of microplankton in the McMurdo Dry Valley Lakes, Antarctica: response to ecosystem legacy or present day climatic controls? Polar Biol. **27**:238–249.
42. **Smith CJ, Osborn AM.** 2009. Advantages and limitations of quantitative PCR (Q-PCR)-based approaches in microbial ecology. FEMS Microbiol. Ecol. **67**:6–20.
43. **Spigel RH, Priscu JC.** 1998. Physical limnology of the McMurdo Dry Valley Lakes, p 153–187. *In* Priscu JC (ed), Ecosystem dynamics in a polar desert: the McMurdo Dry Valleys, Antarctica. Antarctic Research Series, vol 72. American Geophysical Union, Washington, DC.
44. **Steunou AS, et al.** 2006. In situ analysis of nitrogen fixation and metabolic switching in unicellular thermophilic cyanobacteria inhabiting hot spring microbial mats. Proc. Natl. Acad. Sci. U. S. A. **103**:2398–2403.
45. **Strickland JDH, Parsons TR.** 1972. A practical handbook of seawater analysis, vol 167. Fisheries Research Board of Canada, The Alger Press Ltd., Ottawa, Ontario, Canada.
46. **Tabita FR.** 1999. Microbial ribulose 1,5-bisphosphate carboxylase/oxygenase: a different perspective. Photosynth. Res. **60**:1–28.
47. **Tabita FR, Satagopan S, Hanson TE, Kreel NE, Scott SS.** 2008. Distinct form I, II, III, and IV Rubisco proteins from the three kingdoms of life provide clues about Rubisco evolution and structure/function relationships. J. Exp. Bot. **59**:1515–1524.
48. Reference deleted.
49. **Treusch AH, et al.** 2005. Novel genes for nitrite reductase and Amo-related proteins indicate a role of uncultivated mesophilic crenarchaeota in nitrogen cycling. Environ. Microbiol. **7**:1985–1995.
50. **Voytek MA, Priscu J, Ward BB.** 1999. The distribution and relative abundance of ammonia-oxidizing bacteria in lakes of the McMurdo Dry Valley, Antarctica. Hydrobiology **401**:113–130.
51. **Walsh JE.** 2009. A comparison of Arctic and Antarctic climate change, present and future. Antarct. Sci. **21**:179–188.
52. **Ward BB, Priscu JC.** 1997. Detection and characterization of denitrifying bacteria from a permanently ice-covered Antarctic lake. Hydrobiology **347**: 57–68.
53. **Wawrik B, Paul JH, Tabita FR.** 2002. Real-time PCR quantification of *rbcL* (ribulose-1,5-bisphosphate carboxylase/oxygenase) mRNA in diatoms and pelagophytes. Appl. Environ. Microbiol. **68**:3771–3779.
54. **Xu Q, Tabita FR.** 1996. Ribulose-1,5-bisphosphate carboxylase/oxygenase gene expression and diversity of Lake Erie planktonic microorganisms. Appl. Environ. Microbiol. **62**:1913–1920.